Network Curvature as a Geometric Biomarker for Identifying Disease-related Subnetworks.

Marianna Milano[1,3] and Pietro Hiram Guzzi[2,3]

[1] Department of Experimental and Clinical Medicine, Magna Graecia University of Catanzaro, Italy
[2] Department of Medical and Surgical Sciences, Magna Graecia University of Catanzaro, Italy
[3] Data Analytics Research Center, Department of Medical and Surgical Sciences, University Magna Græcia of Catanzaro.
m.milano@unicz.it, hguzzi@unicz.it

Abstract. Biological function emerges from the organization of complex interaction networks spanning multiple scales, from molecular regulation to large-scale brain connectivity. Traditional graph-theoretic descriptors have been widely used to characterize such systems, yet they predominantly encode topological features and often overlook the geometric structure that governs network robustness, redundancy, and resilience to perturbations—properties that are critically altered in disease. Motivated by the need for quantitative descriptors that capture these latent organizational principles, we investigate network curvature as a geometric biomarker for discriminating healthy and pathological biological states. We consider two heterogeneous and conceptually distinct case studies: gene co-expression networks derived from normal and cancer tissues, and whole-brain connectome networks from healthy individuals and patients with major depressive disorder. By leveraging network curvature, we quantify disease-associated alterations in both local cohesiveness and global network organization. Across molecular and neurobiological domains, we observe consistent and systematic curvature shifts distinguishing healthy from diseased networks. These findings support network curvature as a general, domain-independent indicator of biological network dysfunction, highlighting its potential to reveal fundamental geometric signatures of disease that are not captured by conventional connectivity measures.

Keywords: Network Curvature · Biological Network · Brain connectome · Gene co-expression networks.

1 Introduction

Biological systems are intrinsically complex, with function emerging from dense patterns of interactions among molecular and cellular components. These interactions are naturally represented as networks, in which nodes denote biological entities—such as genes, proteins, or brain regions—and edges encode functional

ICCS Camera Ready Version 2026
To cite this paper please use the final published version:
DOI: 10.1007/978-3-032-29912-3_13

or structural relationships. Network-based modeling [19, 16] has therefore become a foundational paradigm in computational biology and neuroscience, enabling the investigation of coordinated regulation, functional integration, and disease-associated reorganization that are difficult to capture with reductionist approaches [26, 11].

At the molecular level, gene co-expression networks [12, 18, 1] provide a powerful framework for characterizing coordinated transcriptional activity across tissues and pathological conditions, revealing disease-associated modules and altered regulatory programs [13, 21]. At the systems neuroscience level, brain connectome networks offer a comprehensive description of large-scale neural organization, supporting the study of cognitive function and neuropsychiatric disorders [3, 22]. In both domains, mounting evidence suggests that disease phenotypes are not driven solely by isolated local perturbations, but rather by widespread reconfiguration of network architecture.

Conventional network analysis [17] has largely relied on topological descriptors such as degree distribution, clustering coefficient, characteristic path length, and modularity. While these measures have proven effective in capturing connectivity patterns and mesoscopic structure, they predominantly reflect local or community-level organization and often fail to encode higher-order structural principles related to robustness, redundancy, and the capacity of networks to sustain function under perturbation [9, 5]. As a consequence, biologically meaningful changes induced by disease—particularly those affecting global organization and resilience—may remain undetected.

These limitations have motivated the introduction of geometric and topological perspectives on network analysis. Among these, discrete notions of Ricci curvature have emerged as a principled approach to quantifying network structure beyond standard graph-theoretic metrics [20, 8]. Network curvature captures how local neighborhoods around connected nodes compare in terms of transport efficiency and cohesion, thereby providing insight into modular organization, information flow, and structural robustness.

In biological contexts, curvature has been shown to correlate with entropy and robustness, and to sensitively reflect disease-associated alterations in network organization. Notably, Tannenbaum et al. [23] demonstrated that cancer-related molecular networks exhibit characteristic curvature signatures linked to increased robustness and functional reprogramming. Subsequent studies have extended these observations to gene regulatory, metabolic, and brain networks, highlighting the ability of curvature-based measures to identify fragile or highly cohesive regions that are not apparent from classical descriptors [6, 7].

Despite these promising results, most existing studies remain confined to individual biological domains or specific diseases, limiting the generality of curvature-based insights. Whether network curvature can serve as a domain-independent biomarker—capable of consistently discriminating healthy and pathological states across heterogeneous biological systems—remains an open and largely unexplored question.

ICCS Camera Ready Version 2026
To cite this paper please use the final published version:
DOI: 10.1007/978-3-032-29912-3_13

Here, we address this gap by investigating network curvature as a unifying geometric marker across two distinct biological scales. Specifically, we analyze (i) gene co-expression networks derived from normal and cancer tissues, constructed from GTEx and TCGA data via the iNetModels 2.0 resource [2, 10, 24], and (ii) brain connectome networks comparing healthy individuals and patients affected by major depressive disorder [14]. By adopting a common curvature-based analytical framework across these molecular and neurobiological systems, we aim to assess whether disease-related network reorganization manifests through consistent geometric signatures, independent of biological scale or domain.

2 Related Work

2.1 Network curvature in complex and biological networks

Discrete curvature measures extend geometric notions of curvature to graphs and metric-measure spaces. Ollivier–Ricci curvature defines curvature through optimal transport between probability measures attached to graph nodes [20]. Forman introduced a combinatorial curvature for cell complexes, which yields an efficient edge-based curvature notion often used as a discrete surrogate in large networks [8]. Variants and graph-specific adaptations of Ricci curvature have also been studied, including formulations tailored to graphs and their analytic properties [15].

In biomedical applications, curvature has been linked to robustness, entropy, and functional organization. Notably, curvature-based analyses have been proposed to characterize alterations in cancer-related networks and to identify network features associated with disease-related changes [23]. These studies suggest that curvature can capture structural signatures not fully described by classical graph descriptors, motivating its use as a discriminative measure.

2.2 Our contribution

Existing work often focuses on a single domain (e.g., cancer networks or a specific brain disorder). In contrast, our paper frames curvature explicitly as a *geometric biomarker* and validates its discriminative role across two heterogeneous biological network types: gene co-expression networks (healthy vs. cancer) and brain connectome networks (healthy vs. depression). This cross-domain validation is intended to strengthen the claim that curvature captures general disease-related geometric reorganization.

ICCS Camera Ready Version 2026
To cite this paper please use the final published version:
DOI: 10.1007/978-3-032-29912-3_13

3 Network Curvature Measures

3.1 Forman–Ricci curvature

For an edge e connecting vertices u and v with weights $w(u)$, $w(v)$, and $w(e)$, the Forman–Ricci curvature can be expressed as:

$$F(e) = w(e)\left(\frac{1}{w(u)} + \frac{1}{w(v)}\right) - \sum_{\substack{e' \sim e \\ e' \neq e}} \frac{w(e)}{\sqrt{w(u')w(v')}}, \tag{1}$$

where $e' \sim e$ denotes edges adjacent to e and u', v' are the endpoints of e'. This measure is computationally efficient and highlights locally dense or fragile edge neighborhoods [8].

3.2 Ollivier–Ricci curvature

Ollivier–Ricci curvature defines curvature using optimal transport between local probability measures on node neighborhoods [20]. For an edge $e = (u, v)$, it can be written as:

$$\kappa(e) = 1 - W_1(\mu_u, \mu_v), \tag{2}$$

where μ_u and μ_v are probability measures associated with nodes u and v, and W_1 is the 1-Wasserstein (Earth Mover's) distance between these measures. Intuitively, positive curvature indicates that the neighborhoods around u and v are similar (locally cohesive structure), while negative curvature often characterizes bridge-like edges connecting distinct modules [20, 15].

4 Case Studies: Network Curvature Across Biological Scales

To assess the ability of network curvature to capture disease-related structural alterations in biological systems, we conducted two complementary case studies spanning distinct biological scales. The first case study focuses on gene co-expression networks, comparing healthy and cancer conditions across multiple human tissues. The second case study investigates brain functional connectivity networks derived from fMRI data, comparing never-depressed and depressed subjects under different experimental conditions. Together, these analyses allow us to evaluate whether curvature consistently reflects pathological network reorganization across molecular and systems-level biological networks. Figure 1 summarises the experimental approach.

4.1 Case Study I: Gene Co-expression Networks (Normal vs. Cancer)

We evaluated curvature on real biological networks from the iNetModels 2.0 database [2], which provides a comprehensive collection of gene co-expression

ICCS Camera Ready Version 2026
To cite this paper please use the final published version:
DOI: 10.1007/978-3-032-29912-3_13

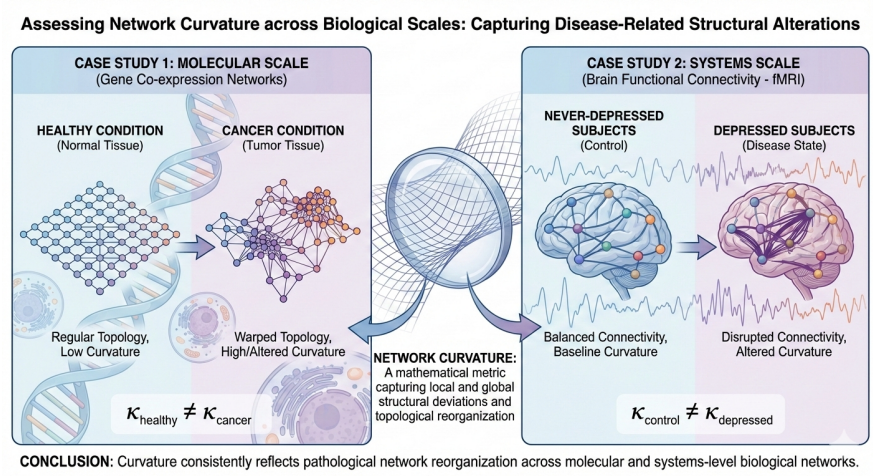

Fig. 1. Cross-Scale Evaluation of Network Curvature in Biological Systems. The research workflow utilizes two distinct case studies to validate network curvature as a biomarker for disease. Case Study 1 (Left) examines molecular-scale gene co-expression networks, identifying topological warping between healthy and cancerous tissues. Case Study 2 (Right) investigates systems-level functional connectivity via fMRI, comparing neural signal organization in never-depressed versus depressed subjects. The central mathematical framework of Network Curvature (κ) serves as the unifying metric to detect pathological reorganization and structural deviations across these diverse biological scales.

ICCS Camera Ready Version 2026
To cite this paper please use the final published version:
DOI: 10.1007/978-3-032-29912-3_13

networks for both normal and cancer conditions. Normal tissue networks were constructed using GTEx data [10], while cancer networks were based on TCGA [4]. The iNetModels resource includes 108 curated, tissue-specific networks representing a broad range of physiological and pathological states.

For this study, we selected 12 representative tissues—*breast, skin, thyroid, lung, pancreas, stomach, colon, prostate, testis, liver, bladder*, and *brain*—spanning both healthy and cancer-associated conditions. The primary structural properties of these networks, including the number of nodes and edges in each condition, are reported in Table 1.

To incorporate geometric information, we computed the Ollivier–Ricci curvature for each edge in the tissue-specific networks under normal and cancer conditions. Ollivier–Ricci curvature quantifies how local network connectivity deviates from an ideal geometric structure: edges with high positive curvature typically correspond to tightly co-expressed gene clusters, while negative curvature marks bridge-like edges connecting distant modules [20, 15]. For each tissue network, we derived node- and network-level summaries, including mean edge curvature and curvature variance, to support quantitative comparisons between healthy and cancer states.

As summarized in Table 2, a consistent decrease in curvature was observed in cancer networks for most tissues, indicating a loss of compactness and modular organization. The largest curvature reductions were found in breast, skin, and pancreas networks, with highly significant differences ($p < 10^{-4}$), reflecting marked topological reorganization. Other tissues, such as lung and bladder, exhibited smaller but still significant changes, suggesting partial preservation of modular structure. The overall distributional shift in curvature between normal and cancer networks across tissues is further illustrated in Figure 2.

Figure 2 shows the distribution of Ollivier–Ricci curvature values in normal and cancer gene co-expression networks across all analyzed tissues. In all cases, cancer networks (red boxplots) exhibit a systematic shift toward lower curvature values compared to their normal counterparts (green boxplots), indicating a loss of local cohesion and modular compactness associated with the disease state. The most pronounced curvature reductions are observed in breast, skin, and pancreas tissues, where cancer networks show a dramatic decrease in both median curvature and overall distribution, corresponding to the largest effect sizes and suggesting extensive disruption of coordinated gene regulation.

4.2 Case Study II: Brain Functional Networks

The second case study investigates whether network curvature can discriminate healthy and pathological brain states using functional connectivity networks derived from fMRI data. We analyzed the publicly available dataset originally published by Lepping *et al.* [14], which includes nineteen subjects diagnosed with Major Depressive Disorder (MDD) and twenty never-depressed (ND) control participants.

During fMRI acquisition, participants listened to standardized emotional auditory stimuli consisting of both musical and nonmusical excerpts with positive

ICCS Camera Ready Version 2026
To cite this paper please use the final published version:
DOI: 10.1007/978-3-032-29912-3_13

Table 1. Structural characteristics of the gene co-expression networks across tissues and conditions. Each network is defined by the number of nodes (genes) and edges (co-expression relationships).

Tissue	Condition	Nodes	Edges
Breast	Normal Tissue	463	52,823
	Cancer Tissue	10,750	61,511
Skin	Normal Tissue	6,294	60,820
	Cancer Tissue	243	17,120
Thyroid	Normal Tissue	4,796	60,226
	Cancer Tissue	5,031	60,140
Lung	Normal Tissue	8,227	60,178
	Cancer Tissue	5,569	60,214
Pancreas	Normal Tissue	4,103	60,327
	Cancer Tissue	710	60,518
Stomach	Normal Tissue	7,372	60,243
	Cancer Tissue	5,389	60,360
Colon	Normal Tissue	5,238	60,211
	Cancer Tissue	60,135	7,733
Prostate	Normal Tissue	8,186	60,394
	Cancer Tissue	5,103	60,155
Testis	Normal Tissue	8,900	60,185
	Cancer Tissue	5,470	60,462
Liver	Normal Tissue	7,798	60,388
	Cancer Tissue	4,001	60,289
Bladder	Normal Tissue	10,750	61,511
	Cancer Tissue	5,292	60,364
Brain	Normal Tissue	1,150	62,311
	Cancer Tissue	4,782	66,164

Table 2. Comparison of curvature (mean ± SD) between Normal and Cancer tissues.

Tissue	Normal (mean ± SD)	Cancer (mean ± SD)	p-value
Breast	0.278 ± 0.065	0.092 ± 0.070	$\mathbf{4.00\times10^{-4}}$
Skin	0.842 ± 0.080	0.116 ± 0.085	$<\mathbf{1.00\times10^{-4}}$
Thyroid	0.648 ± 0.075	0.355 ± 0.070	$\mathbf{1.10\times10^{-3}}$
Lung	0.748 ± 0.070	0.678 ± 0.075	$\mathbf{1.50\times10^{-2}}$
Pancreas	0.764 ± 0.060	0.188 ± 0.065	$<\mathbf{1.00\times10^{-4}}$
Stomach	0.866 ± 0.080	0.666 ± 0.085	$\mathbf{8.00\times10^{-4}}$
Colon	0.900 ± 0.070	0.651 ± 0.075	$\mathbf{6.00\times10^{-4}}$
Prostate	0.761 ± 0.065	0.640 ± 0.070	$\mathbf{2.20\times10^{-3}}$
Testis	0.902 ± 0.055	0.667 ± 0.060	$\mathbf{3.00\times10^{-4}}$
Liver	0.749 ± 0.075	0.547 ± 0.080	$\mathbf{9.00\times10^{-4}}$
Bladder	0.772 ± 0.070	0.654 ± 0.075	$\mathbf{4.50\times10^{-3}}$
Brain	0.680 ± 0.120	0.520 ± 0.130	$\mathbf{1.70\times10^{-3}}$

Table 3. Comparison of Ollivier-Ricci curvature (mean ± SD) between never-depressed (ND) and depressed (MDD) subjects in brain functional networks, under music and non-music experimental conditions.

Condition	ND (mean ± SD)	MDD (mean ± SD)	p-value
Music	0.255 ± 0.019	0.260 ± 0.015	0.033
Non-Music	0.151 ± 0.033	0.144 ± 0.026	0.0430

ICCS Camera Ready Version 2026
To cite this paper please use the final published version:
DOI: 10.1007/978-3-032-29912-3_13

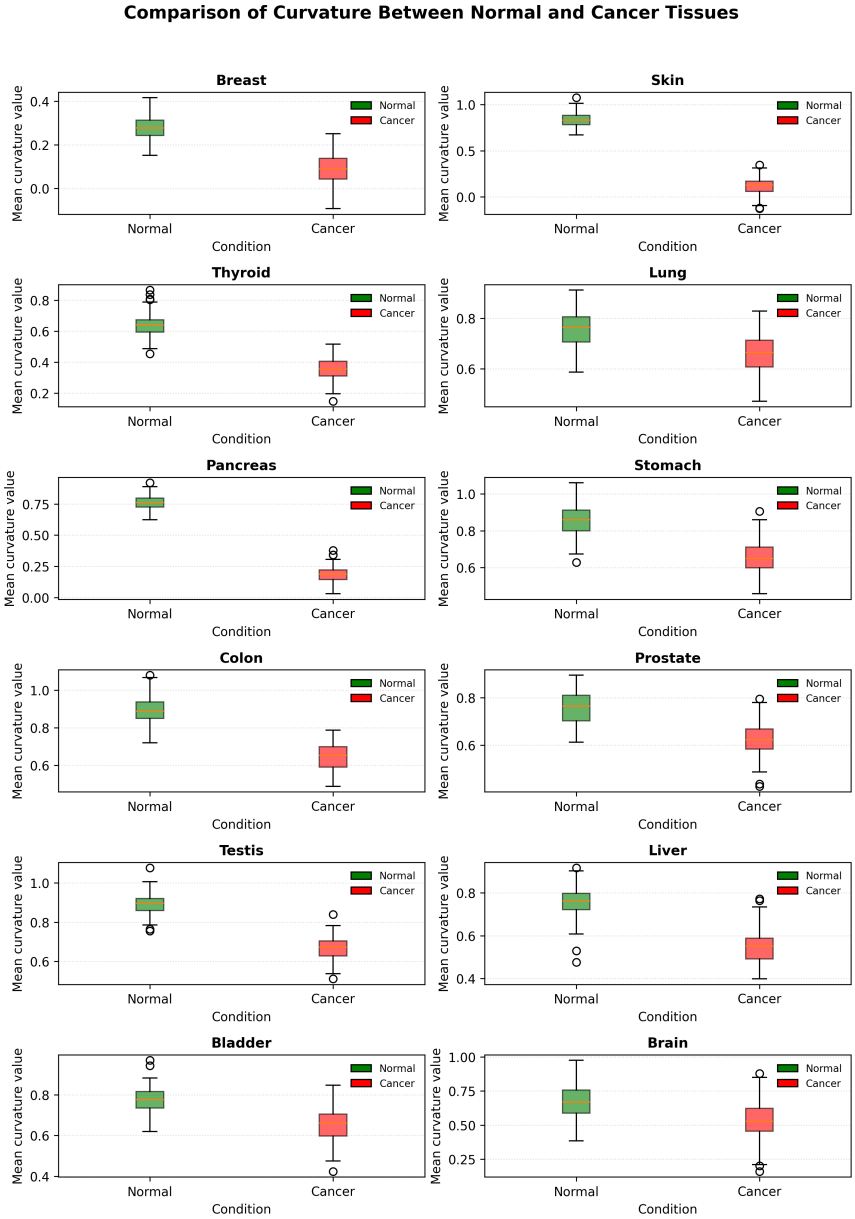

Fig. 2. Distribution of Olivier–Ricci curvature for normal and cancer networks across all tissues. In each box plot, red boxes are cancer tissues, while green refer to normal ones.

ICCS Camera Ready Version 2026
To cite this paper please use the final published version:
DOI: 10.1007/978-3-032-29912-3_13

and negative valence. The musical condition was not intended as a therapeutic intervention, but rather as an experimental stimulus known to engage distributed brain networks involved in emotion processing and cognitive integration. Non musical stimuli were included as a control condition to disentangle music-specific effects from general auditory and emotional processing. Further details on the experimental protocol are provided in the original study [14].

Functional connectivity networks were extracted using the CONN toolbox [25], following the standard preprocessing and analysis pipeline recommended by the authors. Brain parcellation was performed using 164 regions of interest (ROIs), and functional connectivity was estimated using Fisher-transformed Pearson correlation coefficients. For each subject, two functional brain networks were obtained, corresponding to the music and non-music experimental conditions, yielding four categories of networks: ND–Music, MDD–Music, ND–NonMusic, and MDD–NonMusic. All subject-specific brain networks exhibited a highly consistent structure across individuals and conditions, with a fixed number of edges in the non-music condition and a comparable number of nodes across all subjects. Detailed network statistics for each subject are reported in Appendix.

To characterize the geometric organization of brain functional networks, we computed the Ollivier–Ricci curvature on all edges of each subject-specific graph. Curvature values were summarized at the network level by computing the mean curvature per subject. As reported in Table 3, statistically significant differences in curvature were observed between ND and MDD subjects under both experimental conditions. Specifically, curvature was significantly higher in MDD subjects during the music condition ($p = 0.033$), while a significant reduction was observed in the non-music condition ($p = 0.043$). Although effect sizes were modest, the consistency of these differences across conditions suggests a disease-related geometric reorganization of functional brain networks. The distribution of curvature values across groups and conditions is visually summarized in Figure 3.

5 Discussion

In this work, we investigated network curvature as a geometric descriptor of disease-related structural reorganization in biological networks, considering two distinct case studies spanning different biological scales: gene co-expression networks and brain functional connectivity networks. Despite the profound differences in data modality, network size, and biological interpretation, both analyses consistently indicate that curvature captures meaningful alterations in network organization associated with pathological conditions.

In gene co-expression networks, curvature differences between normal and cancer tissues were pronounced and statistically robust across most of the analyzed tissues. Cancer networks systematically exhibited lower Ollivier–Ricci curvature values, indicating a reduction in local cohesion and modular compactness. This behavior is consistent with the widespread transcriptional deregula-

ICCS Camera Ready Version 2026
To cite this paper please use the final published version:
DOI: 10.1007/978-3-032-29912-3_13

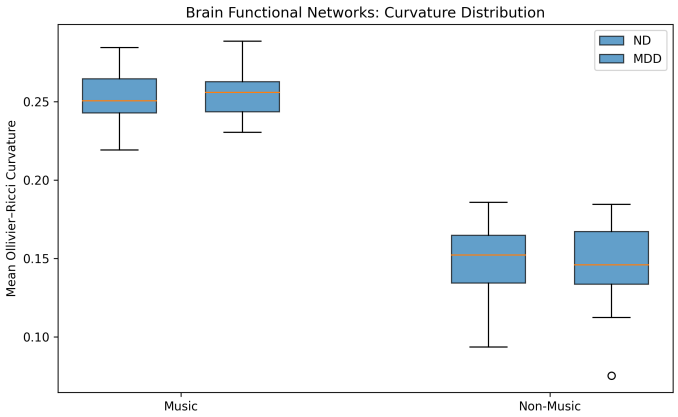

Fig. 3. Distribution of mean Ollivier–Ricci curvature in subject-specific brain functional networks. Boxplots compare never-depressed (ND) and depressed (MDD) subjects under music and non-music experimental conditions.

tion observed in cancer, where normal regulatory modules become fragmented and inter-module connectivity increases. The observed curvature reductions reflect a loss of geometric compactness in the network, suggesting that curvature is sensitive to large-scale topological reorganization at the molecular level.

In contrast, curvature differences in brain functional networks were more subtle but remained statistically significant between never-depressed (ND) and Major Depressive Disorder (MDD) subjects under both music and non-music experimental conditions. While effect sizes were modest, the consistency of curvature differences across conditions indicates that the observed geometric alterations are not stimulus-specific but instead reflect disease-related functional reorganization. This result is in line with the known complexity of neuropsychiatric disorders, where pathological effects often manifest as distributed and compensatory network changes rather than as large global disruptions. The ability of curvature to capture these subtle geometric deviations highlights its suitability for probing higher-order organization in brain functional networks.

Importantly, the two case studies reveal a scale-dependent yet conceptually consistent behavior of curvature. In gene co-expression networks, disease effects manifest as large shifts in average curvature, reflecting extensive transcriptional reorganization. In brain networks, disease-related alterations emerge as smaller but reproducible geometric deviations that remain detectable across experimental conditions. This observation suggests that curvature provides a common geometric perspective for characterizing network reorganization across biological scales, while naturally adapting to domain-specific manifestations of pathology.

From a methodological standpoint, curvature captures structural information that goes beyond purely topological descriptors commonly used to summarize network connectivity. While classical measures such as edge density or average

ICCS Camera Ready Version 2026
To cite this paper please use the final published version:
DOI: 10.1007/978-3-032-29912-3_13

connectivity primarily reflect the quantity of connections in a network, curvature has been shown to encode local geometric properties related to neighborhood cohesion, robustness, and information flow [20, 7]. In the present study, curvature highlights disease-associated network reorganization that is not directly apparent from node or edge counts alone, supporting its role as a complementary descriptor of network structure.

Overall, the empirical evidence provided by the two case studies supports the interpretation of network curvature as a candidate geometric biomarker of disease-related network alterations. Rather than serving as a diagnostic or predictive clinical marker, curvature should be viewed as a structural signature that reflects underlying changes in network organization. Its ability to detect large-scale disruptions in cancer gene networks and subtler, yet statistically significant, alterations in brain functional connectivity highlights its potential as a biologically interpretable descriptor of network reorganization in complex biological systems.

Several limitations should be acknowledged. The present analyses are cross-sectional and based on moderate sample sizes, particularly in the neuroimaging case study. Future work should investigate curvature-based descriptors in longitudinal settings, explore multivariate curvature representations, and assess robustness across independent datasets and alternative network construction strategies. Nonetheless, the consistency of curvature-related effects across molecular and systems- level networks provides strong evidence for the relevance of geometric network analysis in the study of disease-related biological reorganization.

6 Conclusions

This study demonstrates that network curvature captures disease-related structural reorganization in biological networks across distinct domains and scales. By analyzing gene co-expression networks and brain functional connectivity networks, we showed that curvature consistently reflects alterations in network geometry associated with pathological states. In gene networks, curvature robustly discriminated healthy and cancer conditions, while in brain networks it revealed statistically significant, yet subtler, differences between never-depressed and depressed subjects.

Our findings indicate that curvature functions as a domain-agnostic geometric descriptor capable of identifying both large-scale and fine-grained network alterations. Rather than serving as a standalone clinical biomarker, network curvature should be considered a *candidate network-based geometric biomarker* that provides mechanistic insight into how disease reshapes biological connectivity. The cross-scale consistency observed in this work suggests that curvature-based approaches may contribute to a unified framework for studying robustness, modularity, and functional reorganization in complex biological systems.

Future research should focus on integrating curvature with multivariate and machine learning approaches, extending analyses to longitudinal data, and ex-

ICCS Camera Ready Version 2026
To cite this paper please use the final published version:
DOI: 10.1007/978-3-032-29912-3_13

ploring its complementarity with established network metrics. Overall, this work highlights the value of geometric network analysis as a principled and interpretable tool for advancing our understanding of disease-related network dynamics.

Acknowledgments. This work has been partially supported by the OFIDIAPlus (Operational Fire Danger preventIon plAtform Plus) project under the INTERREG GREECE-ITALY 2021-2027 PROGRAMME.
This work has been partially supported by the "HeartTrack: Driving the Patient Journey in Heart Failure" project funded by PR CALABRIA FESR FSE 2021 – 2027.

Disclosure of Interests. The authors have no competing interests to declare that are relevant to the content of this article.

References

1. Agapito, G., Cannataro, M., Cinaglia, P., Milano, M.: Ten practical tips and tricks to improve the effectiveness of biological network alignment. PLOS Computational Biology **21**(9), e1013386 (2025)
2. Arif, M., Zhang, C., Li, X., Güngör, C., Çakmak, B., Arslantürk, M., Tebani, A., Özcan, B., Subaş, O., Zhou, W., et al.: inetmodels 2.0: an interactive visualization and database of multi-omics data. Nucleic acids research **49**(W1), W271–W276 (2021)
3. Bullmore, E., Sporns, O.: Complex brain networks: graph theoretical analysis of structural and functional systems. Nature Reviews Neuroscience **10**(3), 186–198 (2009)
4. Cancer Genome Atlas Research Network: The cancer genome atlas pan-cancer analysis project. Nature Genetics **45**(10), 1113–1120 (2013). https://doi.org/10.1038/ng.2764
5. Cannataro, M., Guzzi, P.H., Veltri, P.: Impreco: Distributed prediction of protein complexes. Future Generation Computer Systems **26**(3), 434–440 (2010)
6. Chatterjee, T., DasGupta, B., Albert, R.: A review of two network curvature measures. Nonlinear Analysis and Global Optimization pp. 51–69 (2021)
7. Farooq, H., Chen, Y., Georgiou, T.T., Tannenbaum, A.: Network curvature as a hallmark of brain structural connectivity. Nature Communications **8**, 1–13 (2017). https://doi.org/10.1038/s41467-017-01566-8
8. Forman, R.: Bochner's method for cell complexes and combinatorial ricci curvature. Discrete & Computational Geometry **29**, 323–374 (2003). https://doi.org/10.1007/s00454-002-0743-x
9. Fortunato, S.: Community detection in graphs. Physics Reports **486**(3-5), 75–174 (2010)
10. GTEx Consortium: The genotype-tissue expression (GTEx) project. Nature Genetics **45**(6), 580–585 (2013). https://doi.org/10.1038/ng.2653
11. Guzzi, P.H., Milenković, T.: Survey of local and global biological network alignment: the need to reconcile the two sides of the same coin. Briefings in bioinformatics **19**(3), 472–481 (2018)
12. Guzzi, P.H., Roy, A., Milano, M., Veltri, P.: Non parametric differential network analysis: a tool for unveiling specific molecular signatures. BMC bioinformatics **25**(1), 359 (2024)

ICCS Camera Ready Version 2026
To cite this paper please use the final published version:
DOI: 10.1007/978-3-032-29912-3_13

13. Guzzi, P.H., Roy, S.: Biological network analysis: Trends, approaches, graph theory, and algorithms. Elsevier (2020)
14. Lepping, R.J., Atchley, R.A., Chrysikou, E.G., Martin, L.E., Clair, A.A., Ingram, R.E., Simmons, W.K., Savage, C.R.: Neural processing of emotional musical and nonmusical stimuli in depression. PLOS ONE **11**(6), e0156859 (2016). https://doi.org/10.1371/journal.pone.0156859
15. Lin, Y., Lu, L., Yau, S.T.: Ricci curvature of graphs. Tohoku Mathematical Journal, Second Series **63**(4), 605–627 (2011)
16. Milano, M., Cinaglia, P., Cannataro, M., Guzzi, P.H.: Biological community detection with graph neural network and network curvature analysis on gene co-expression networks. In: International Conference on Computational Science. pp. 285–296. Springer (2025)
17. Milano, M., Cinaglia, P., Guzzi, P.H., Cannataro, M.: A novel local alignment algorithm for multilayer networks. Informatics in Medicine Unlocked **44**, 101425 (2024). https://doi.org/https://doi.org/10.1016/j.imu.2023.101425, https://www.sciencedirect.com/science/article/pii/S235291482300271X
18. Milano, M., Cinaglia, P., Guzzi, P.H., Cannataro, M.: A computational approach to study age-related modifications of the genes involved in parkinson's disease. Computers in Biology and Medicine **196**, 110765 (2025)
19. Milano, M., Guzzi, P.H.: Novel graph neural network method for differential network analysis in biological data. In: Proceedings of the 16th ACM International Conference on Bioinformatics, Computational Biology, and Health Informatics. pp. 1–1 (2025)
20. Ollivier, Y.: Ricci curvature of markov chains on metric spaces. Journal of Functional Analysis **256**(3), 810–864 (2009). https://doi.org/10.1016/j.jfa.2008.11.001
21. Sonawane, A.R., Platig, J., Fagny, M., Chen, C.Y., Paulson, J.N., Lopes-Ramos, C.M., DeMeo, D.L., Quackenbush, J., Glass, K., Kuijjer, M.L.: Understanding tissue-specific gene regulation. Cell reports **21**(4), 1077–1088 (2017)
22. Sporns, O.: Network attributes for segregation and integration in the human brain. Current Opinion in Neurobiology **23**(2), 162–171 (2013). https://doi.org/10.1016/j.conb.2012.11.015
23. Tannenbaum, A., Sander, C., Sandhu, R., Zhu, L., Kolesov, I., Reznik, E., Senbabaoglu, Y., Georgiou, T.: Graph curvature and the robustness of cancer networks. arXiv preprint arXiv:1502.04512 (2015)
24. Weinstein, J.N., Collisson, E.A., Mills, G.B., Shaw, K.R., Ozenberger, B.A., Ellrott, K., Shmulevich, I., Sander, C., Stuart, J.M.: The cancer genome atlas pan-cancer analysis project. Nature genetics **45**(10), 1113–1120 (2013)
25. Whitfield-Gabrieli, S., Nieto-Castanon, A.: Conn: a functional connectivity toolbox for correlated and anticorrelated brain networks. Brain connectivity **2**(3), 125–141 (2012)
26. Zitnik, M., Li, M.M., Wells, A., Glass, K., Morselli Gysi, D., Krishnan, A., Murali, T., Radivojac, P., Roy, S., Baudot, A., et al.: Current and future directions in network biology (2024)

Appendix.Supplementary Tables Table 4 reports the structural properties of all subject-specific brain functional networks under music and non-music conditions. These data are provided for completeness and confirm the consistency of network construction across subjects and experimental conditions.

ICCS Camera Ready Version 2026
To cite this paper please use the final published version:
DOI: 10.1007/978-3-032-29912-3_13

Table 4. Structural characteristics of subject-specific brain functional networks. For each subject, two networks were extracted corresponding to music and non-music experimental conditions.

Subject	Clinical Condition	Network Type	Nodes	Edges
sub-01	ND	Non-Music	160	2005
sub-01	ND	Music	164	4901
sub-02	ND	Non-Music	154	2005
sub-02	ND	Music	164	4866
sub-03	ND	Non-Music	163	2005
sub-03	ND	Music	164	4867
sub-04	ND	Non-Music	158	2005
sub-04	ND	Music	166	4926
sub-05	ND	Non-Music	157	2005
sub-05	ND	Music	164	4981
sub-06	ND	Non-Music	156	2006
sub-06	ND	Music	164	4701
sub-07	ND	Non-Music	157	2005
sub-07	ND	Music	164	4821
sub-08	ND	Non-Music	134	2005
sub-08	ND	Music	163	5120
sub-09	ND	Non-Music	161	2005
sub-09	ND	Music	164	4864
sub-10	ND	Non-Music	161	2005
sub-10	ND	Music	164	5122
sub-11	ND	Non-Music	160	2005
sub-11	ND	Music	164	4524
sub-12	ND	Non-Music	158	2005
sub-12	ND	Music	164	4839
sub-13	ND	Non-Music	156	2005
sub-13	ND	Music	164	4948
sub-14	ND	Non-Music	157	2005
sub-14	ND	Music	164	4900
sub-15	ND	Non-Music	163	2005
sub-15	ND	Music	164	4797
sub-16	ND	Non-Music	148	2005
sub-16	ND	Music	164	4926
sub-17	ND	Non-Music	162	2005
sub-17	ND	Music	164	4710
sub-18	ND	Non-Music	160	2005
sub-18	ND	Music	164	4999
sub-19	ND	Non-Music	160	2005
sub-19	ND	Music	164	4887
sub-20	ND	Non-Music	165	2005
sub-20	ND	Music	164	4717
sub-21	MDD	Non-Music	159	2005
sub-21	MDD	Music	164	4781
sub-22	MDD	Non-Music	159	2005
sub-22	MDD	Music	163	5066
sub-23	MDD	Non-Music	164	2005
sub-23	MDD	Music	163	5112
sub-24	MDD	Non-Music	162	2005
sub-24	MDD	Music	164	4917
sub-25	MDD	Non-Music	163	2005
sub-25	MDD	Music	164	4802
sub-26	MDD	Non-Music	157	2005
sub-26	MDD	Music	164	4906
sub-27	MDD	Non-Music	153	2005
sub-27	MDD	Music	164	4903
sub-28	MDD	Non-Music	161	2005
sub-28	MDD	Music	164	5000
sub-29	MDD	Non-Music	161	2005
sub-29	MDD	Music	163	5075
sub-30	MDD	Non-Music	163	2005
sub-30	MDD	Music	164	4672
sub-31	MDD	Non-Music	163	2005
sub-31	MDD	Music	164	5213
sub-32	MDD	Non-Music	152	2005
sub-32	MDD	Music	164	4901
sub-33	MDD	Non-Music	162	2005
sub-33	MDD	Music	164	4942
sub-34	MDD	Non-Music	162	2005
sub-34	MDD	Music	164	4933
sub-35	MDD	Non-Music	150	2005
sub-35	MDD	Music	164	5089
sub-36	MDD	Non-Music	161	2005
sub-36	MDD	Music	163	5002
sub-37	MDD	Non-Music	147	2005
sub-37	MDD	Music	161	5158
sub-38	MDD	Non-Music	160	2005
sub-38	MDD	Music	164	4847
sub-39	MDD	Non-Music	160	2005
sub-39	MDD	Music	164	5460

ICCS Camera Ready Version 2026
To cite this paper please use the final published version:
DOI: 10.1007/978-3-032-29912-3_13